

Wideband Circularly Polarized Microstrip Antenna With Wide Beamwidth

Lei Chen, *Member, IEEE*, Tian-Ling Zhang, Chao Wang, and Xiao-Wei Shi, *Senior Member, IEEE*

Abstract—A novel wideband circularly polarized antenna for S-band satellite communications with wide beamwidth is presented. The wide impedance bandwidth is achieved by using the modified inverted-L feeds and stacked patches. The wide beamwidth is obtained by the semi-open metal cavity. A prototype of the antenna is implemented, and the measured bandwidth is 30.1% with the reflection coefficient ≤ -10 dB, axial ratio ≤ 3 dB, half-power beamwidth (HPBW) $\geq 100^\circ$, and gain ≥ 3 dBi. Experimental results show that the proposed antenna has good impedance matching, circular polarization, and wide beamwidth characteristics.

Index Terms—Circular polarization, semi-open metal cavity, wide beamwidth, wideband.

I. INTRODUCTION

WITH the rapid development in wireless applications such as mobile communication systems, radars, and satellite systems, circularly polarized (CP) antennas have drawn wide attraction [1]–[4]. CP antennas can alleviate multipath effects and provide flexibility in the orientation angle between transmitting and receiving antennas.

Many CP microstrip antennas have been designed such as antennas with dual-fed-type or four-fed-type structure and various kinds of slot antennas [5]–[7]. Compared to traditional CP antennas, microstrip antennas are widely used because of relatively inexpensive cost and easy design. Meanwhile, microstrip antennas with wide beamwidth, wide band, and low profile are urgently required for satellite wireless systems [8]. Cavity-backed CP microstrip antennas with wide beamwidth characteristic are very attractive candidates that can provide excellent CP coverage, although the operating bandwidth is less than 14% because of the high *Q*-factor of cavity structure [9]–[12].

In this letter, a modified cavity-backed CP microstrip antenna is proposed for S-band Mobile Satellite Service (MSS) networks with the desired half-power beamwidth (HPBW) greater than 100° . The modified inverted-L feeds, stacked patches, and semi-

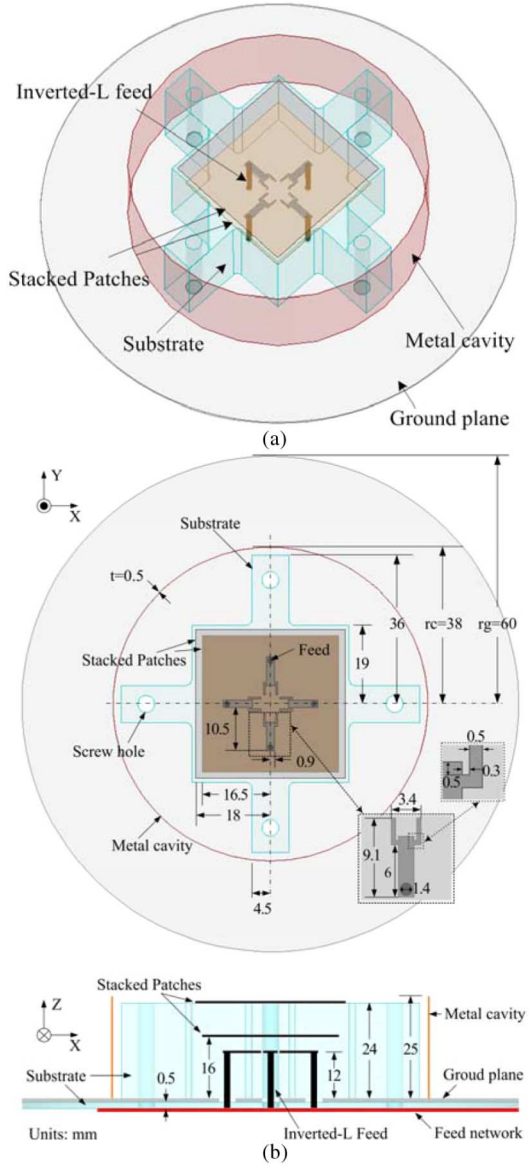


Fig. 1. Geometry of the proposed antenna. (a) 3-D view. (b) Top view and side view.

Manuscript received July 01, 2014; accepted July 17, 2014. Date of publication July 21, 2014; date of current version August 22, 2014. This work was supported by the National Natural Science Foundation of China under Grant 61072021 and the National Key Laboratory Funds.

The authors are with the National Laboratory of Science and Technology on Antennas and Microwaves, Xidian University, Xi'an 710071, China (e-mail: leichen@mail.xidian.edu.cn; tianlingzhang@126.com; wangchaoxidian@163.com; xwshixd@sina.com).

Color versions of one or more of the figures in this letter are available online at <http://ieeexplore.ieee.org>.

Digital Object Identifier 10.1109/LAWP.2014.2341241

open metal cavity structure are used to widen impedance bandwidth and beamwidth at the same time. Without increasing the profile of the antenna, a relative bandwidth of 30.1% for HPBW above 100° has been achieved. The performance of the antenna is simulated using ANSYS HFSS and validated by experiment.

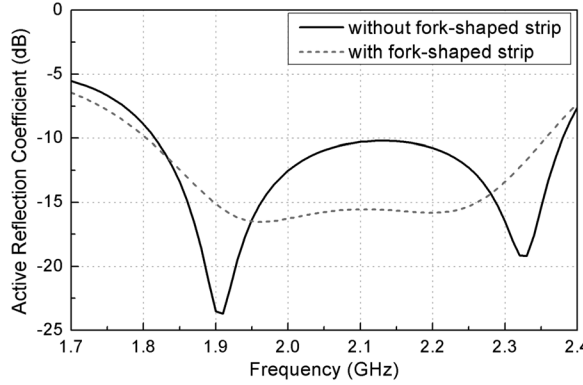


Fig. 2. Comparison of simulated active reflection coefficient of the proposed antenna with and without fork-shaped strip.

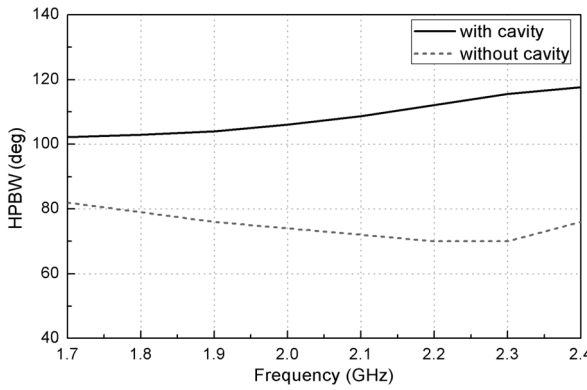


Fig. 3. Comparison of simulated HPBW between the proposed antenna with and without the cavity.

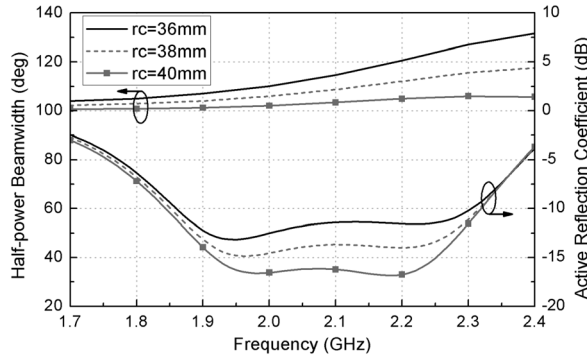


Fig. 4. Simulated HPBW and active reflection coefficient of the proposed antenna according to the variation of the cavity intern radius.

II. ANTENNA CONFIGURATION AND DESIGN

A. Antenna Design

A prototype of the proposed antenna is fabricated on a low-loss substrate with a relative permittivity of 2.65, and the total dimension of the antenna is $120 \times 120 \times 25.5 \text{ mm}^3$. The geometry of the proposed microstrip antenna is shown in Fig. 1 where the 3-D, top, and side views are given. The antenna is designed as a stacked patch antenna fed by four fork-shaped inverted-L feeds that are used to achieve wideband impedance bandwidth. Meanwhile, those four inverted-L feeds, which can increase the capacitance of feeding structure and realize good symmetrical

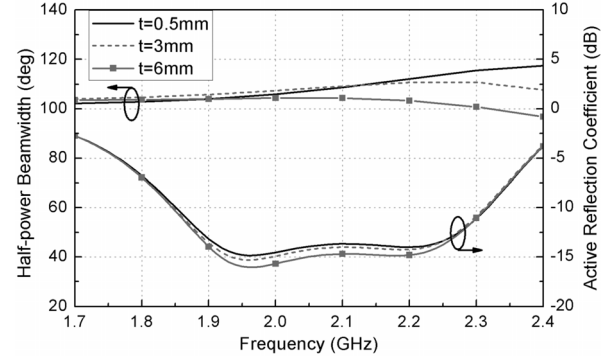


Fig. 5. Simulated HPBW and active reflection coefficient of the proposed antenna according to the variation of the cavity thickness.

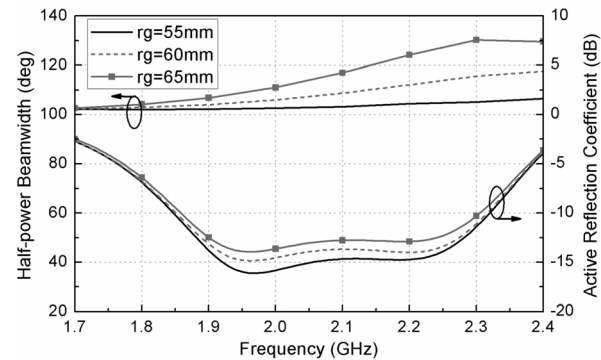


Fig. 6. Simulated HPBW and active reflection coefficient of the proposed antenna according to the variation of the ground plane radius.

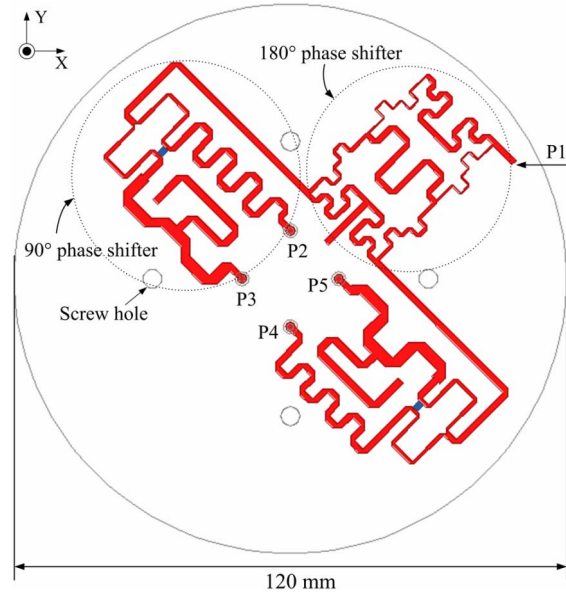


Fig. 7. Geometry of feed network of the proposed antenna.

circularly polarized radiation patterns, are located symmetrically along the antenna center line with the excited phase of 0° , 90° , 180° , and 270° , respectively. Fig. 2 shows the simulated results of active reflection coefficient with and without the fork-shaped strip. It can be found that this structure can improve the impedance characteristics efficiently. The substrate is composed of a square-shaped and a cross-shaped substrate that can

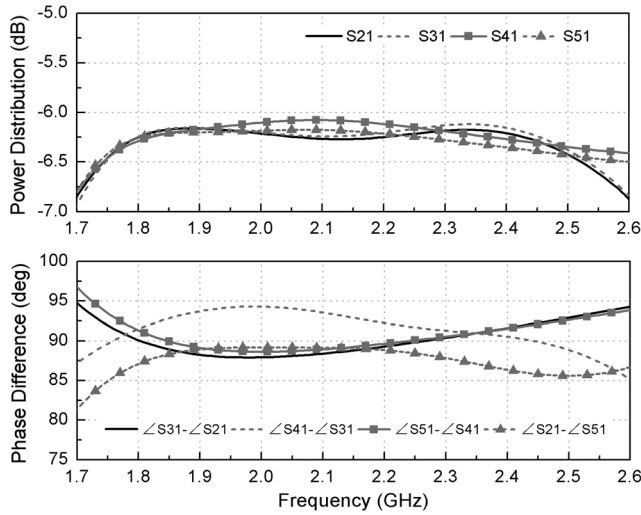


Fig. 8. Simulated power distributions at the output ports and phase differences between the consecutive output ports (P2 to P5).

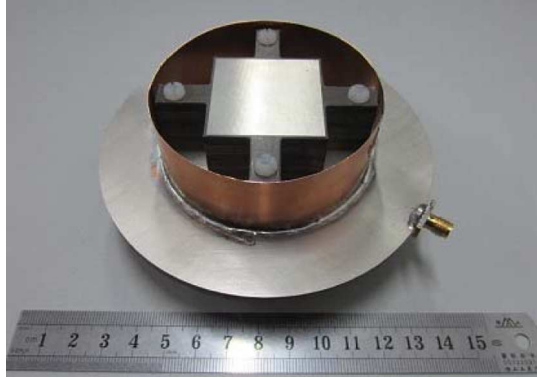


Fig. 9. Photograph of the proposed antenna.

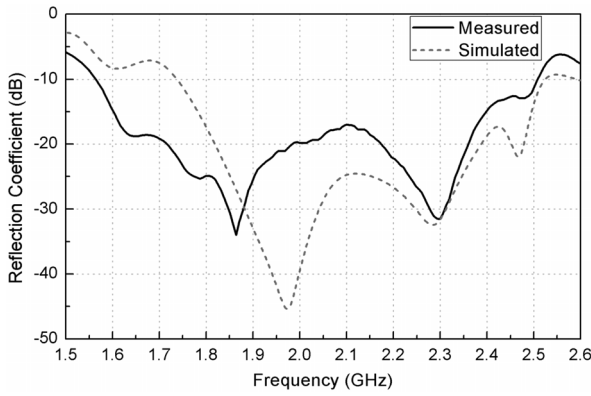


Fig. 10. Measured and simulated reflection coefficient of the proposed antenna.

be easily fixed with the feed network by screws. The height of substrate is 24 mm to broaden the impedance bandwidth.

To broaden the HPBW of the antenna over the operating band, the hollow cylinder is placed around the antenna, which can form a semi-open metal cavity. A comparison of simulated HPBW between the proposed antenna with and without the cavity is shown in Fig. 3. It is observed that the cavity can significantly broaden the beamwidth of the antenna. By introducing the cavity, the HPBW is greater than 100°.

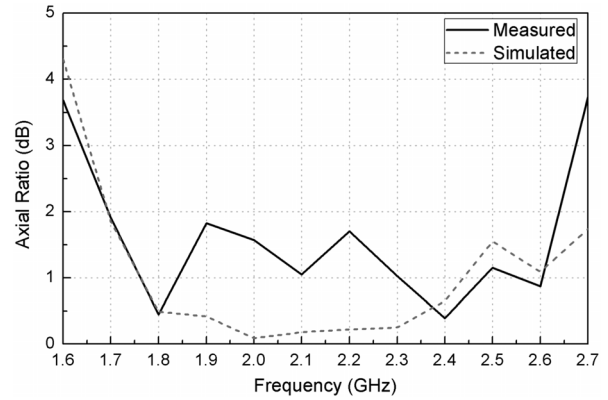


Fig. 11. Measured and simulated axial ratio of the proposed antenna.

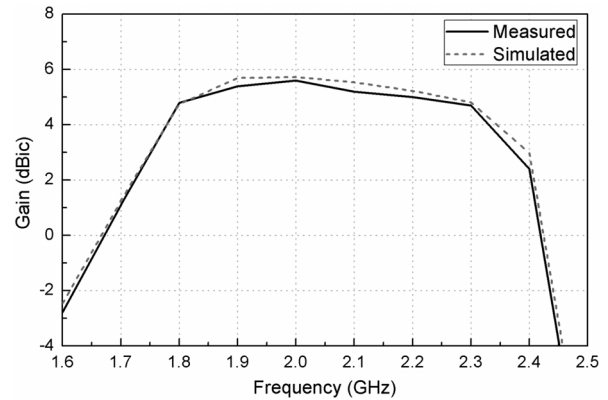


Fig. 12. Measured and simulated gain of the proposed antenna.

To characterize the proposed antenna, parametric studies have been carried out using ANSYS HFSS. The simulated HPBW and active reflection coefficient for different values of the cavity intern radius are shown in Fig. 4. The HPBW decreases especially clearly at higher frequency with the cavity intern radius increasing, and the impedance characteristic is improved at the same time. Fig. 5 illustrates the influence of the cavity thickness on the HPBW and active reflection coefficient. It can be observed that the HPBW decreases at higher frequency with the cavity thickness increasing, and the impedance characteristic is not sensitive to the change of the thickness. The ground plane size usually affects the antenna performance. Fig. 6 shows the simulated HPBW and active reflection coefficient for different values of the ground plane radius. With the ground plane radius enlarging, the HPBW increases especially at higher frequency, and the impedance characteristic deteriorates slightly.

B. Feed Network

With the purpose of obtaining good wideband circular polarization characteristic, equal input power with relative 90° phase difference in turn should be provided to the four inverted-L feeds. Fig. 7 shows the geometry of wideband feed network whose output ports (P2 to P5) are connected with inverted-L feeds. The feed network is composed of a fractal miniaturized 180° phase shifter, which is illustrated in detail in [13], and two wideband 90° phase shifters [14]. Fig. 8 shows the simulated

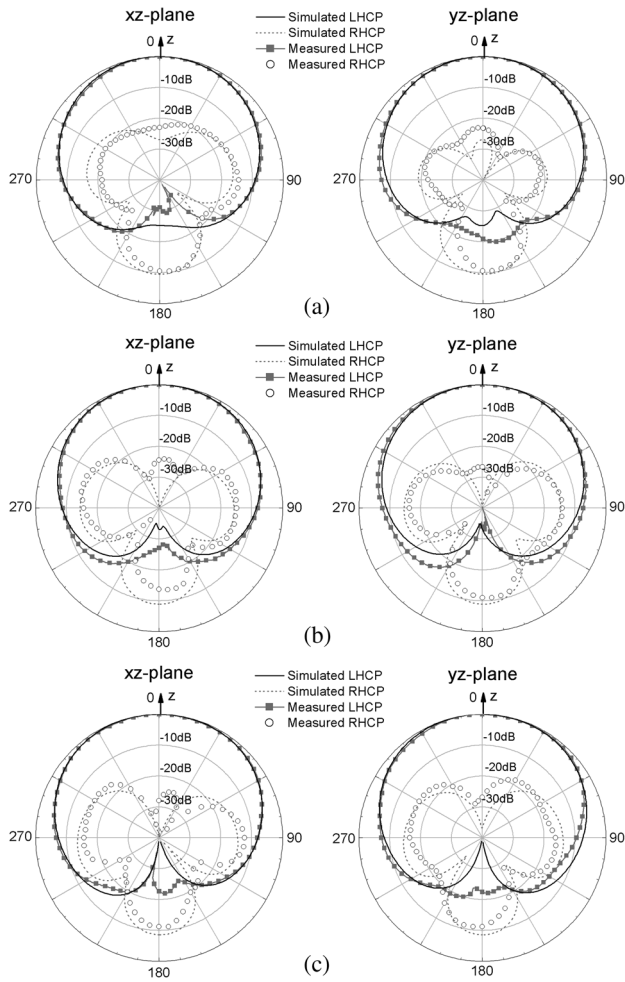


Fig. 13. Measured and simulated radiation patterns in two principal planes. (a) At 1.75 GHz. (b) At 2.1 GHz. (c) At 2.35 GHz.

amplitude and phase responses. It is found that the feed network can provide nearly equal amplitude and $90^\circ \pm 5^\circ$ phase difference to the output ports over a frequency range of 1.78–2.5 GHz. Meanwhile, the insertion losses of the feed network are not significant, ensuring that the antenna has good radiation efficiency.

III. EXPERIMENTAL RESULTS

The proposed antenna has been fabricated as shown in Fig. 9. The reflection coefficient was measured by Agilent E8363B vector network analyzer. Fig. 10 shows the measured reflection coefficient in comparison to the simulated one. The measured 10-dB reflection coefficient bandwidth is about 46% from 1.57 to 2.51 GHz, which is similar to the simulated one. The measured and simulated axial ratio bandwidths are given in Fig. 11. The proposed antenna exhibits a measured 3-dB axial-ratio bandwidth of 47.2% from 1.65 to 2.67 GHz. Fig. 12 shows the measured and simulated results for the gain. It is seen that the measured gain bandwidth is 30.1% from 1.75 to 2.37 GHz for gain ≥ 3 dBic.

The measured and simulated radiation patterns in two principal planes (xz - and yz -planes) at 1.75, 2.1, and 2.35 GHz are

presented in Fig. 13 and show that the antenna is left-hand circularly polarized. These results are in good agreement especially in terms of HPBWs. The measured HPBWs vary from 102° to 120° , which confirms the wide beamwidth property of the antenna. Moreover, the axial ratio is below 4 dB within the HPBW at each frequency.

On the basis of the common bandwidth for the reflection coefficient ≤ -10 dB, axial ratio ≤ 3 dB, HPBW $\geq 100^\circ$, and gain ≥ 3 dBic, the proposed CP antenna exhibits an approximate bandwidth of 30.1% from 1.75 to 2.37 GHz. The measured results show a significant enhancement in impedance bandwidth and beamwidth due to using modified inverted-L feeds, stacked patches, and semi-open metal cavity structure.

IV. CONCLUSION

The design of wide impedance bandwidth and beamwidth circularly polarized antenna has been presented. Using fork-shaped inverted-L feeds, stacked patches, and semi-open metal cavity, the proposed design exhibits 30.1% relative bandwidth taking into account of 10-dB reflection coefficient, gain, HPBW, and 3-dB axial ratio. The proposed antenna with wide impedance bandwidth and wide beamwidth characteristics can be a good candidate for mobile satellite terminal applications.

REFERENCES

- [1] I. Gonzalez, J. Gomez, A. Tayebi, and F. Catedra, "Optimization of a dual-band helical antennas for TTC applications at S-band," *IEEE Antennas Propag. Mag.*, vol. 54, no. 4, pp. 63–77, Aug. 2012.
- [2] E. C. Choi, J. W. Lee, and T. K. Lee, "Modified S-band satellite antenna with isoflux pattern and circularly polarized wide beamwidth," *IEEE Antennas Wireless Propag. Lett.*, vol. 12, pp. 1319–1322, 2013.
- [3] Y. M. Pan and K. W. Leung, "Wideband circularly polarized dielectric bird-nest antenna with conical radiation pattern," *IEEE Trans. Antennas Propag.*, vol. 61, no. 2, pp. 563–570, Feb. 2013.
- [4] K. L. Chung, "High-performance circularly-polarized antenna array using metamaterial-line based feed network," *IEEE Trans. Antennas Propag.*, vol. 61, no. 12, pp. 6233–6237, Dec. 2013.
- [5] K. L. Lau and K. M. Luk, "A novel wide-band circularly polarized patch antenna based on L-probe and aperture-coupling techniques," *IEEE Trans. Antennas Propag.*, vol. 53, no. 1, pp. 577–580, Jan. 2005.
- [6] A. Khidre, K. F. Lee, A. Z. Elsherbeni, and F. Yang, "Wide band dual-beam U-slot microstrip antenna," *IEEE Trans. Antennas Propag.*, vol. 61, no. 3, pp. 1415–1418, Mar. 2013.
- [7] X. L. Bao and M. J. Ammann, "Dual-frequency Dual-sense circularly-polarized slot antenna fed by microstrip line," *IEEE Trans. Antennas Propag.*, vol. 56, no. 3, pp. 645–649, Mar. 2008.
- [8] J. J. H. Wang, "Antennas for global navigation satellite system (GNSS)," *Proc. IEEE*, vol. 100, no. 7, pp. 2349–2355, Jul. 2012.
- [9] C. A. Lindberg, "A shallow-cavity UHF crossed-slot antenna," *IEEE Trans. Antennas Propag.*, vol. AP-17, no. 5, pp. 558–563, Sep. 1969.
- [10] E. Jorgensen, B. K. Nielsen, O. Breinbjerg, and M. Lumholt, "A cavity-backed crossed-slot antenna element for an S-band circular polarization spherical coverage satellite antenna system," in *Proc. Int. Symp. Antennas Propag.*, Fukuoka, Japan, Aug. 2000, vol. 1, pp. 361–364.
- [11] J. E. Pallesen, O. Kim, and O. Breinbjerg, "Augmentation of crossed-slot antenna with inverted-L wires for enhancement of hemispherical coverage," *Electron. Lett.*, vol. 42, no. 15, pp. 836–837, Jul. 2006.
- [12] F. Manshadi, "End-loaded crossed-slot radiating elements," *IEEE Trans. Antennas Propag.*, vol. 39, no. 8, pp. 1237–1240, Aug. 1991.
- [13] M. Caillet, M. Clénet, A. Sharaiha, and Y. M. M. Antar, "A compact wide-band rat-race hybrid using microstrip lines," *IEEE Microw. Wireless Compon. Lett.*, vol. 19, no. 4, pp. 191–193, Apr. 2009.
- [14] S. Y. Zheng, W. S. Chan, and K. F. Man, "Broadband phase shifter using loaded transmission line," *IEEE Microw. Wireless Compon. Lett.*, vol. 20, no. 9, pp. 498–500, Sep. 2010.